

Theoretical study of structure and energetics of gold clusters with the EAM method

Denitsa Alamanova: Physical and Theoretical Chemistry, University of Saarland, Bld. B2
2, 66123 Saarbrücken, Germany
Tel: +49-681-302-3809, Fax: +49-681-302-3857, E-Mail: deni@springborg.pc.uni-sb.de

Valeri G. Grigoryan: Physical and Theoretical Chemistry, University of Saarland, Bld. B2
2, 66123 Saarbrücken, Germany
Tel: +49-681-302-4420, Fax: +49-681-302-3857, E-Mail: vg.grigoryan@mx.uni-saarland.de

Michael Springborg: Physical and Theoretical Chemistry, University of Saarland, Bld. B2
2, 66123 Saarbrücken, Germany
Tel: +49-681-302-3856, Fax: +49-681-302-3857, E-Mail: m.springborg@mx.uni-saarland.de

Keywords: Gold clusters, embedded-atom-method calculations, structure, stability

MS-ID:

vg.grigoryan@mx.uni-saarland.de

February 6, 2008

Heft: x/x (x)

Received: x Accepted: x

Abstract

Using the Embedded Atom Method as developed by Voter and Chen in combination with the *variable metric/quasi-Newton* and our own *Aufbau/Abbau* methods, we have identified the three most stable isomers of Au_N clusters with N up to 150. For the first time clusters with tetrahedral symmetry are found to form the ground states of Au_{17} and Au_{34} . The Au_{54} *icosahedron* without a central atom and the Au_{146} *decahedron* are found to be particularly stable, whereas the highly symmetric second and third Mackay icosahedra that could have been obtained for $N = 55$ and 147, respectively, do not correspond to the particularly stable structures. The three lowest-lying isomers of Au_{55} and Au_{147} are low-symmetrical structures. Various structural and energetic properties are analysed, such as stability function, occurrence of magic-sized clusters, construction of icosahedral and *fcc* shells, and cluster growth.

Widmung

This work is dedicated to Prof. Dr. Wolf Weyrich, Physical Chemistry, University of Konstanz, Germany, on the occasion of his 65th birthday.

1 Introduction

Since the first part of the 20th century it has been recognized that theoretical studies can constitute an important ingredient of science, first through the dedication of chairs to the field of theoretical physics and later through the establishment of chairs in theoretical chemistry. Simultaneously, by defining ‘theory’ as an independent part of science, the interactions between theory and experiment have in many cases been reduced. Persons who unite these two parts are, therefore, of immense importance and, simultaneously, able to contribute to science in a way that is unmatched by most colleagues. A person, occupying a chair of physical chemistry, and being active in both experimental and theoretical studies of the properties of matter, is, accordingly, unique. Such a person is Wolf Weyrich, who has made significant contributions to the understanding of the properties of a large range of systems, going all the way from smaller molecules to extended solids. In the later years his interests have also turned towards the properties of nanoparticles that somehow lie in between the materials of his earlier interests. Metal nanoparticles are thereby of central interest. Therefore, it is with pleasure that we dedicate the present work to Wolf Weyrich on the occasion of his 65th birthday.

Clusters form an important link between isolated atoms and molecules at one extreme and bulk solids at the other. Their large surface-to-volume ratio gives them unique physical and chemical properties. On the other hand, the combination of finite with large size makes it difficult to characterize and analyze their properties in detail. From a theory point of view the central difficulty lies in the determination of the structure of the system of interest and only through comparison with experimental information more definite statements about their properties can be made.

Gold clusters represent some of the mostly studied clusters (for a detailed discussion, see Ref. [1, 2]). They have recently been investigated in connection with the synthesis of nanostructured materials and devices [3, 4, 5, 6, 7]. Their structural and energetic properties have been studied with High-Resolution Electron Microscopy (HREM) and various spectroscopic techniques [8, 9, 10, 11, 12, 13, 14, 15, 16, 17, 18, 19, 20, 21, 22, 23, 24, 25]. Literature concerning small Au_N clusters is enriched with numerous investigations based on density-functional methods [26, 27, 28, 29, 30, 31, 32, 33, 34, 35, 36, 37, 38, 39, 40, 41, 43, 42, 44] that are not yet capable of giving a definite answer to the problem at what cluster size the structural 2D – 3D transition occurs. Recent studies combining theory and experiment [45, 46, 47, 48] show that the gold clusters are planar at least up to $N = 7$ for Ref. [46], or up to $N = 12$, according to Häkkinen [45] and Furche *et al.* [47].

However, global structure optimization is difficult when using *ab initio* methods already at very small cluster sizes. Nevertheless, some studies in this direction exist. Thus, the authors of Ref. [27, 39] performed density functional calculations on clusters containing more than 30 atoms,

relaxing selected high-symmetric configurations. Alternatively, the global optimizations of larger clusters are all based on approximate methods like molecular dynamics [49, 50, 51, 52, 53, 54, 55, 56, 57, 58, 59, 60] and semiempirical potentials like the EAM [13, 61, 62], Sutton-Chen [63], Murrell-Mottram [64, 65], or the many-body Gupta potential [66, 67, 68, 69, 70, 71]. Using these methods, unbiased structure optimizations were performed up to the 80-atom cluster. Medium-sized clusters ($80 \leq N \leq 150$) have hardly been studied. Besides the first-principles study of Häberlen *et al.* [27] and the EAM calculations by Cleveland *et al.* [13, 61, 62] considering particular structural motifs, there exists essentially no further investigation on the clusters in this size range.

In most of the studies, special attention is paid to the so-called ‘magic-numbered’ clusters, that possess closed electronic and/or geometric shells. Various studies on the smallest ‘magic’ cluster Au_{13} have identified the formation of an icosahedron [26, 27, 63, 64, 69, 71]. Only the authors of Ref. [34, 35] found a disordered structure as the lowest-lying isomer for this cluster size. On the other hand, semiempirical potentials [61, 63, 64, 71] and the density functional study by Häkkinen *et al.* [29] on the Au_{38} cluster predict the truncated octahedron to be the global minimum for this cluster size. However, on the basis of first-principles and Gupta potential calculations, the authors of Ref. [68, 70] state that a disordered structure is actually lower in energy than the symmetric. Ultimately, it may be suggested that the obtained structure depends sensitively on the type of the potential, since by using another form of the same potential, Darby *et al.* [71] found a truncated octahedral structure to be the global minimum of Au_{38} . The situation is more clear for the Au_{55} and Au_{75} clusters, where a disordered structure [63, 66, 67, 69, 70, 71] or a Marks decahedron (m-D_{5h}) [67, 69] seem to constitute the global minima.

Several groups have performed calculations on larger clusters by minimizing the total energy of initially chosen symmetric structures, although it may be feared that the structures may not be those of the global total-energy minima. Moreover, only few cluster sizes were studied — the octahedral Au_{79} [61, 63] and Au_{140} [61], the decahedral Au_{101} , Au_{116} , and Au_{146} [61], and the icosahedral Au_{147} [27, 61]. The structures and energetics of the clusters between these high symmetrical ones remain scarcely investigated.

The purpose of the present study is to carry out unbiased calculations on small and intermediate gold clusters, and, subsequently, to investigate the occurrence of magic clusters and the growth patterns, especially for larger clusters. To our knowledge, two earlier studies on gold clusters with the same version of EAM have been performed previously, i.e., the work of Rey and coworkers [72, 73] and that of Sebetci and Güvenç [74]. The first study considered only the energetics and stability of small gold clusters ($2 \leq N \leq 23$). Sebetci *et al.* used a basin-hopping Monte Carlo minimization approach to find the global minima of Al_N , Au_N , and Pt_N clusters with $N \leq 80$. The total energies, point groups, and structural

assignments were presented.

In the present study the structure and energetics of the three most stable isomers of small and medium-sized Au_N clusters with $2 \leq N \leq 150$ have been determined for each cluster size by using a combination of the embedded-atom method in the version of Voter and Chen [78, 79, 80], the *variable metric/quasi-Newton* method, and our own *Aufbau/Abbau* method. The paper is organized as follows. In Sec. 2 we briefly outline the embedded-atom method, and in Sec. 3 we present our structural-determination methods. The main results are given in Sec. 4, and a brief summary is offered in Sec. 5.

2 The Embedded Atom Method

The main idea of the EAM was initially presented by Daw, Baskes, and Foiles (DBF) [75, 76, 77] in 1983–1986, and since then the generality of the functions of the EAM of DBF has been successfully tested through numerous applications to different systems of metals and alloys, including defects, surface and interface structures, surface and bulk phonons, etc. In a previous paper [81] we reported results for the global minima of Ni_N , Cu_N , and Au_N clusters with up to 60 atoms, obtained with two different versions of the EAM. There we discussed the incapability of the so-called DBF version of EAM to describe properly the properties of the smallest gold clusters, which could be related to the parameterization of the potential only to bulk properties. The version developed by Voter and Chen [78, 79, 80] takes into account also the properties of the dimer, which makes this method more suitable for the description of the smallest clusters. Accordingly, in this study we use this version of the EAM for the calculation of the total energy of a given cluster.

The principle of the method is to split the total energy of the system into a sum over atomic energies:

$$E_{tot} = \sum_i^N E_i. \quad (1)$$

The embedding energy is obtained by considering each atom as an impurity embedded into a host provided by the rest of the atoms. The electron-electron interaction is presented as sums of short-ranged, pair potentials. Accordingly,

$$E_{tot} = \sum_i F_i(\rho_i^h) + \frac{1}{2} \sum_{i \neq j} \phi_{ij}(r_{ij}) \quad (2)$$

where ρ_i^h is the local electron density at site i , F_i is the embedding energy, i.e., the energy required to embed an atom into this density, and ϕ_{ij} is a short-range potential between atoms i and j separated by distance r_{ij} .

The pair potential, according to the Voter-Chen version, is taken to be a Morse potential,

$$\phi(r) = D_M[1 - e^{-\alpha_M(r-R_M)}]^2 - D_M \quad (3)$$

where the three parameters, D_M , R_M , and α_M , define depth, position of the minimum, and a measure of the curvature at the minimum, respectively. The local density at site i is assumed being a superposition of atomic electron densities:

$$\rho_i^h = \sum_{j \neq i} \rho_j^a(r_{ij}) \quad (4)$$

where $\rho_j^a(r_{ij})$ is the spherically averaged atomic electron density provided by atom j at the distance r_{ij} . The density function is taken as the density of a hydrogenic 4s orbital:

$$\rho(r) = r^6[e^{-\beta r} + 2^9 e^{-2\beta r}] \quad (5)$$

where β is an adjustable parameter. Because $r^6 e^{-\beta r}$ turns over at short r , the second term has been added to maintain the monotonically decreasing character of $\rho(r)$ at shorter r . This 4s orbital density, appropriate for Ni and Cu, also works well for gold. To ensure that the interatomic potential and its first derivatives are continuous, both $\phi(r)$ and $\rho(r)$ are cut off at $r=r_{\text{cut}}$. In the fitting procedure, the five parameters defining $\phi(r)$ and $\rho(r)$ (D_M , R_M , α_M , β_M and r_{cut}) are optimized by minimizing the root-mean-square deviation between the calculated and reference properties of different selected systems like molecules, surfaces, solids, and defects. Because $F(\rho^h)$ is redefined for each choice of the parameters, the potential always gives perfect agreement with experimental values such as a_0 , E_{coh} and the bulk modulus B . The reference properties are the three cubic elastic constants (C_{11} , C_{12} and C_{44}), the unrelaxed vacancy formation energy (E_{vac}^f), and the bond length (R_e) and bond strength (D_e) of the diatomic molecule. The values of ρ_i^a , ϕ_{ij} and $F_i(\rho_i)$ that were used by the Voter-Chen version, are available in numerical form for Ni, Pd, Pt, Cu, Ag, Au and Al.

Our reason for choosing the EAM was dictated by the good agreement to experiment, as well as to first principles calculations, and last but not least by the high computational efficiency allowing one to investigate clusters with more than 100 atoms without severe constraints on the initial geometry, which is impossible with first principles methods. In a previous work [81] we performed calculations on smaller gold clusters with $2 \leq N \leq 60$ atoms comparing the EAM of Daw, Baskes, and Foiles (DBF) and the version used in this work, and we found that the DBF overestimated the binding energy of the dimer by 209% and underestimated the bond distance by 37%. For comparison, the EAM of Voter and Chen gives dimer binding energy corresponding to 99.6% of the experimental value,

and bond distance that is 92.2% of the experimental value. For this reason we chose to work with the Voter-Chen version that describes correctly the dimer properties.

3 Structure optimization

Using expression (1) we can calculate the total energy of any cluster with any structure as a function of structure, i.e., of the atomic coordinates $\{\vec{R}_i\}$, $E_{\text{tot}}(\vec{R}_1, \vec{R}_2, \dots, \vec{R}_N)$. In order to obtain the closest local total-energy minimum we use the *variable metric/quasi-Newton* method [83].

For searching the global minima we have developed our own *Aufbau/Abbau* method that is described in details in previous works [84, 85]. It consists of the following steps:

1) We consider two cluster sizes with N and $N + K$ atoms with $K \simeq 5 - 10$. For each of those we randomly generate and relax a large set of structures, from which those with the lowest total energy are selected.

2) One by one, each of the N atoms is displaced randomly, and the closest local minima is determined. If the new structure has a lower total energy than the original one, this new one is kept, and the old one discarded. This is repeated approximately 1000 – 2000 times depending on cluster size.

3) This leaves us with two ‘source’ clusters, Au_N and Au_{N+K} with their lowest total energies. One by one an atom is added at a random position to the structure with N atoms (many hundred times for each size), and the structures are relaxed. In parallel, one by one an atom is removed from the structure with $N + K$ atoms — for each intermediate cluster with N' atoms we consider all $N' + 1$ possible configurations, that one can obtain by removing one atom from the $\text{Au}_{N'+1}$ cluster. From the two series of structures for $N \leq M \leq N + K$ those structures of the lowest energies are chosen and these are used as seeds for a new set of calculations. First, when no lower total energies are found in the two sets of calculations, it is assumed that the structures of the global-total-energy minima have been identified.

4 Results and Discussion

4.1 Small gold clusters

Like all other semiempirical potentials, the one of the embedded-atom method does not include explicitly the electrons and their orbitals. Therefore, such a potential tends to prefer high-symmetry, compact structures, whereas structures of lower symmetry that can be explained through electronic effects are not found. As a result, for the smallest gold clusters, where spin-orbit interactions play an important role, our global-minima structures are compact (see Table 1), and the planar structures (that are

believed to be those of the true total-energy minima) only metastable. In the size range $N = 4 - 7$ first principles studies obtain these 3D configurations as higher-lying isomers, which can serve as an example of how the inclusion of electronic effects can change the energetic ordering of the isomers. On the other hand, the addition of electronic effects in the semiempirical potentials would restrict their use only to small and relatively larger clusters with pre-chosen structures. An appropriate choice in this respect could be the Density Functional Tight-Binding methods (DFTB) that include explicitly the electrons and are computationally more efficient than the common density functionals. Actually, in a recent study [82] we demonstrated the important role that the electronic effects can play for the binding energy and the stability functions. However, except for $N = 4$, where a rhombus was the lowest-lying isomer according to the DFTB method, all the ground state structures for the smallest gold clusters $\text{Au}_5 - \text{Au}_9$ had 3D shapes. On the other hand, even the most recent density-functional studies are still not in agreement at which cluster size the structural transition 2D - 3D occurs. According to the LDA study of Wang *et al.* [35], it is the pentagonal bipyramid that forms the global minimum of Au_7 . Remacle and Kryachko [44] suggested that gold clusters are planar at least up to $N = 9$, while Walker [43] predicted that the transition occurs at Au_{11} . Using ion mobility measurements and *ab-initio* molecular dynamics Kappes *et al.* [46, 47] found that the 3D transitions occur at Au_{12}^- and Au_8^+ . The same group studied the adsorption of CO on isolated gold cluster cations in the size range $N = 1 - 65$. The smallest clusters with $4 \leq N \leq 6$ as well as Au_8 were found to be planar, while for Au_7 the global minimum was a 3D structure, but not a bipyramid, in contrast to the results of Wang *et al.* [35]. In a combined experimental and theoretical study Häkkinen and coworkers [45] confirmed the 2D - 3D transition at Au_{12}^- , however, Xiao and Wang [42] suggested that for the neutral clusters this transition occurs first at Au_{15} . In most of the cases the planar structures are competing with 3D isomers, and the energetic differences are insignificant, which in turn means that the ordering of the isomers depends strongly on the used functional and the starting conditions. For example, Häkkinen *et al.* [33] compared the global minima of relativistic and nonrelativistic Au_7^- clusters and found that for the nonrelativistic gold the lowest-lying isomer was a capped octahedron that corresponds to our second isomer for this cluster size. At larger cluster sizes the potential used in this study yields results in agreement with density-functional and experimental studies. The study of Häkkinen *et al.* [29] on the Au_{38} cluster predicted the truncated octahedron to be the global minimum, and a recent experiment [25] showed that the Au_{55}^- cluster most probably is not an icosahedron, but a structure with a low symmetry, in agreement with our results.

In summary, we can conclude that although our results for the smallest gold clusters correspond to higher-lying isomers within the first principles methods, due to the lack of electronic effects, our method is sufficiently

accurate in describing the larger gold clusters with $N > 9$, where most probably the planar structures begin to compete with 3D configurations.

4.2 Energetic properties

The high stability of the so-called ‘magic-numbered’ clusters has become a subject of great interest in connection with its relevance in the medicinal and the colloidal chemistry, as well as in the production of catalysts and high-tech nanomaterials.

In Fig. 1 we show the binding energy per atom for the global-minima structures, as well as the difference between the total energies of the lowest-lying isomers obtained by us and those found by Sebetci *et al.* [74] using exactly the same potential for the interatomic interactions. One can see that the latter difference increases almost linearly with the number of atoms and has its maximum at $N = 79$, where we obtained a truncated octahedron in contrast to the structure with D_{3h} symmetry found by Sebetci and Güvenç. Except for few cases, the total-energy difference is marginal (about 5 meV/atom, which may be due to numerical differences), giving support for the quality of both theoretical approaches in optimizing the structure. At $N = 52$ they obtained an uncentered icosahedron-like structure with C_{2h} symmetry, that lies energetically between our second and third lowest isomers.

In order to identify the particularly stable clusters we have considered the following criteria. The clusters can be considered as very stable if their binding energy per atom is much larger than that of the two neighboring clusters. This can be quantified through the stability function, $E_{\text{tot}}(N + 1.1) + E_{\text{tot}}(N - 1.1) - 2E_{\text{tot}}(N.1)$, where $E_{\text{tot}}(N.k)$ is the total energy of the energetically k -lowest isomer of the Au_N cluster. This function, that has maxima for particularly stable clusters, is shown in Fig. 2. Here we can identify a large number of particularly stable clusters, i.e., so-called magic clusters. These are found for $N = 4, 6, 10, 13, 15, 17, 23, 28, 30, 36, 38, 40, 42, 45, 49, 54, 58, 61, 64, 66, 68, 73, 75, 77, 79, 82, 84, 89, 92, 95, 101, 109, 111, 116, 118, 124, 128, 133, 135, 140, 144$, and 146. The most pronounced peaks (marked in the figure) occur at $N = 13, 30, 40, 54, 75, 79, 82, 124, 133, 140$, and 146. In agreement with Sebetci and Güvenç [74], the 54-atom icosahedron without a central atom is found to represent a magic-numbered cluster, whereas the Au_{55} cluster does not. The latter possesses a distorted icosahedral structure with C_{3v} symmetry, lying 0.374 eV lower than the perfect icosahedron, 2.9 eV lower than the decahedron, and 3.27 eV lower than the cuboctahedron. In our study, all the three lowest-lying isomers of Au_{55} have lower energy than the symmetric structures, in agreement with previous studies where disordered configurations were found as global minima for Au_{55} [66, 67, 70, 71]. For Au_{38} and Au_{75} , a cuboctahedron [29, 63, 64, 71, 74] and a Marks decahedron [63, 67, 69, 74] were obtained, in agreement with first-principles and semiempirical studies. However, two studies employing

the many-body Gupta potential identified amorphous structures as those of the global minima of Au₃₈ [68, 70], which is most probably due to the parameterization of the potential, since Darby *et al.* [71] found an octahedron as the lowest-lying isomer by using another version of the same potential.

Another striking result of our study is that the 146-atom Marks decahedron represents a peak in the stability function, whereas the Au₁₄₇ icosahedron does not. According to our study, the third Mackay icosahedron lies 2.89 eV lower than the cuboctahedron, which in turn is 2.53 eV lower than the decahedron, but 0.37 eV higher than a disordered structure with partly decahedral construction. To our knowledge, this is the first study predicting a disordered global minimum for the Au₁₄₇ cluster.

According to our other criterion for a particularly stable cluster, such a cluster occurs if the energy difference between the two energetically lowest isomers $E_{\text{tot}}(N.2) - E_{\text{tot}}(N.1)$ is large. This energy difference is shown in Fig. 3, and comparing to Fig. 2 we can see that many of the clusters that are particularly stable according to the first criterion are stable also according to the second one.

4.3 Structural properties

In this subsection, instead of discussing in particular the structures of the individual clusters, we shall introduce different quantities that are devised to reduce the available information to some few key numbers. The theoretical background of the descriptors used in this subsection was introduced by us in a previous work [85].

The shape analysis, based on the eigenvalues of the matrix with the moments of inertia and whose results are shown in Fig. 4, separates the clusters into being overall spherical, more cigar-like shaped, or more lens-like shaped. One can see that only few clusters have a spherical shape (these are found for the energetically lowest isomer for $N = 4, 6, 13, 17, 34, 38, 54, 79$, and 140 , and for the next one for $N = 42$ and 116), all of them corresponding to high-symmetrical isomers (cf. Table 1) and, for the lowest-energy isomer, most of them to the class of magic clusters. It is interesting that the average value follows more or less the same curve for all the three isomers, with some deviations at $N = 130, 146$, and 147 . Also the largest differences show a similar behaviour, except for some few cases mainly for N below 40 and between 80 and 85. Therefore, except when the eigenvalues are all very similar (which occurs for N around 50, 70, 100, 116, and 140), the overall shape (i.e., lens- or cigar-like) is the same for all three isomers.

The construction of atomic shells can be easily seen from the distribution of radial distances (i.e., the distance for each individual atom to the center of mass) shown in Fig. 5 for the ground state structures as function of the cluster size. Up to N around 50, no trends can be identified, with an exception around $N = 13$. But for N just above 50 a

clear tendency towards shell construction can be seen for the first isomer. This corresponds to the formation of the Au_{54} icosahedral cluster. Also for N close to 110 and around 140 shell constructions for the lowest-lying isomer are observed. In the latter case, this corresponds to the formation of an octahedron. The radial distributions for the second and the third isomers are not shown, as they are quite similar to that for the first isomer. Particular shell constructions are found only for highly symmetrical clusters corresponding to $N = 42, 48, 80, 101, 116$, and around Au_{130} for the second isomer, and around $N = 40, 60, 116$, and 130 for the third isomer.

In Fig. 6 we show the average and minimal coordination numbers and the average bond lengths of the clusters. We define two atoms as being bonded if their interatomic distance is less than 3.49 Å, which is the average value between the nearest-neighbour distance (2.89 Å) and the next-nearest-neighbour distance (4.08 Å) in bulk Au. Moreover, we distinguish between inner atoms with a coordination number of 12 or larger and surface atoms with a coordination number less than 12.

Fig. 6(a) presents the average coordination number as a function of N . A saturation towards the bulk limit of 12 is seen, although one has to remember that even for the largest cluster of our study 94 out of 150 atoms are characterized as surface atoms. Also, the function increases in general with the size of the system, with oscillations in particular for the clusters with $N = 17$ and 18, which is due to the formation of a tetrahedron for Au_{17} , and a structure with C_{4v} symmetry at $N = 18$, respectively. The latter has already earlier been obtained with the EAM method (see Ref. [74]), but it is the first time that a tetrahedral configuration is found for the Au_{17} cluster.

The minimum atomic coordination for each cluster size is shown in Fig. 6(b). The existence of low-coordinated atoms, i.e. with coordination numbers of 3 or 4, could point to the occurrence of a cluster growth, where extra atoms are added to the surface of the cluster, whereas higher coordination numbers could indicate a growth where atoms are inserted inside the cluster, or, alternatively, upon a strong rearrangement of the surface atoms. The latter is the case for the gold clusters, with few exceptions at $N = 14, 17, 18, 78, 83$, and 134, where lower coordinations are found. The lowest coordination corresponding to Au_{14} is in connection with the formation of an icosahedron plus one additional atom on the surface. At $N = 17$ and 18, some structural changes take place, as discussed above. Au_{78} and Au_{83} correspond to structures with a decahedral motif capped with one additional atom. This is also the case for Au_{134} where the C_{2v} symmetry of the decahedral structure corresponding to $N = 133$ is lowered by the addition of an atom to the surface.

Fig. 6(c) shows the average bond length as a function of the cluster size. The dashed line corresponds to the bulk value of 2.89 Å. The average bond length for all the structures is smaller than the bulk value, especially for Au_{17} and Au_{18} , where more compact structures are formed. However, this

property approaches the bulk value faster than the average coordination number.

One important issue in many of the molecular dynamics studies on gold clusters is to identify how the clusters grow and if the cluster with N atoms could be derived from the one with $N - 1$ atoms simply by adding one atom. In order to quantify this possibility we use the concept of similarity functions, introduced by us earlier [84, 85].

The similarity function S , shown in Fig. 7(a), approaches 1 if the Au_N cluster is very similar to the Au_{N-1} cluster plus an extra atom. We see indeed that for N up to around 50, S is significantly different from 1, confirming that in this range the growth is complicated. The most pronounced peaks occur at $6 < N < 9$, $15 < N < 20$, 34, 38, 39, 52, 56, 79, 80, 85, 111, 126, 140, 141, and $145 < N < 147$. Many of these correspond to highly symmetrical clusters, however some of the clusters with larger peaks ($N = 39, 56, 62, 85, 111, 126, 141$, and 145) have lower symmetry. The octahedral Au_{38} and the low-symmetrical Au_{39} are structurally very different from their $N-1$ -atom neighbours. Au_{56} marks the end of the icosahedral shell built between Au_{52} and Au_{55} , and the clusters resume their disordered growth. The octahedral Au_{61} is followed by the disordered Au_{62} , and the decahedral Au_{85} comes after the disordered Au_{84} . Between the decahedral Au_{110} and Au_{112} lies the disordered Au_{111} . The addition of one atom to the disordered Au_{125} leads to the formation of an unfinished but regular decahedron at $N = 126$. The decahedral Au_{141} comes immediately after the octahedron corresponding to $N = 140$. Although Au_{144} has partly decahedral construction, its $N+1$ -atom neighbour is disordered. It seems that for each cluster size there is a rearrangement of the gold atoms, and no particular growth motif can be identified. This, in turn, means that the cluster growth is very complicated and it is difficult to consider it as an one-by-one atom addition.

Finally, some selected, high-symmetry clusters are shown in Fig. 8.

5 Summary and Conclusions

We have determined the three energetically lowest isomers of gold clusters in the range $2 \leq N \leq 150$ by using a combination of the embedded-atom method in the version of Voter and Chen (for the calculation of the total energy for a given structure), the *variable metric/quasi-Newton* method (for the determination of the closest total-energy minimum), and our own *Aufbau/Abbau* method (for the determination of the global total-energy minimum). Although the calculations provide a large amount of information for each individual cluster, instead of discussing each cluster separately, we focused on identifying general trends such as total energy per atom, overall symmetry and shape, average bond length and coordination number, and similarity with $N - 1$ -atom clusters.

The version of EAM used in the present calculations is parameterized

to bulk, as well as to the dimer properties, which allows it to describe properly the properties of the smaller gold clusters.

This study predicts a number of particularly stable clusters, i.e., ‘magic-numbered’ clusters that in many cases are in agreement with results obtained by first principles and other semiempirical studies when such exist, but the advantage of our study is that the structures were obtained by using a completely unbiased approach. These magic numbers were clearly visible both in the ‘stability function’ and in the total-energy difference between the energetically lowest and higher-lying isomers.

We also found that even for our largest clusters the binding energy per atom has still not converged to the bulk limit. Similarly, the average coordination number is far from the bulk value, but higher than for nickel clusters, where several structures with shell constructions and corresponding low coordination numbers were formed [85]. The average bond distance for gold has not reached the bulk value, due to the rearrangement of the atoms for each cluster size that leads to the formation of very compact structures.

The shape analysis showed that roughly spherical clusters corresponded mainly to the energetically lowest isomer, but in some cases also to the second-lowest one, and that these often belong to particularly stable structures.

By analysing the distribution of radial distances as a function of the cluster size we could identify a region with N around 55, where a shell construction was formed. Comparing to previous results for nickel clusters [85], where clear shell constructions were formed at N around 13, 55, and 147, here the atoms rearrange for each global minimum, and therefore particular shell constructions can not be observed. The similarity function also points to the lack of regular growth.

6 Acknowledgments

We gratefully acknowledge *Fonds der Chemischen Industrie* for the very generous support. This work was supported by the SFB 277 of the University of Saarland and by the German Research Council (DFG) through project Sp439/14-1. Finally, it is a pleasure to dedicate this work to Wolf Weyrich who, through his work, demonstrated to one of the present authors (MS) the importance of combining theory and experiment.

References

- [1] P. Pyykkö, *Angew. Chem. Int. Ed.* **43**, 4412 (2004).
- [2] F. Baletto and R. Ferrando, *Rev. Mod. Phys.* **77**, 371 (2005).

- [3] R. L. Whetten, J. T. Khoury, M. M. Alvarez, S. Murthy, I. Vezmar, Z. L. Wang, P. W. Stephens, C. L. Cleveland, W. D. Luedtke, and U. Landman, *Adv. Mater.* **8**, 428 (1996).
- [4] A. Sanchez, S. Abbet, U. Heiz, W. -D. Schneider, H. Häkkinen, R. N. Barnett, and U. Landman, *J. Phys. Chem. A* **103**, 9573 (1999).
- [5] H. Häkkinen, S. Abbet, A. Sanchez, U. Heiz, and U. Landman, *Angew. Chem. Int. Ed.* **42**, 1297 (2003).
- [6] L. D. Socaciu, J. Hagen, T. M. Bernhardt, L. Wöste, U. Heiz, H. Häkkinen, and U. Landman, *J. Am. Chem. Soc.* **125**, 10437 (2003).
- [7] U. Heiz and E. L. Bullock, *J. Mater. Chem.* **14**, 564 (2004).
- [8] K. J. Taylor, C. L. Pettiette-Hall, O. Cheshnovsky, and R. E. Smalley, *J. Chem. Phys.* **96**, 4 (1992).
- [9] H. Handschuh, G. Ganteför, P. S. Bechthold, and W. Eberhardt, *J. Chem. Phys.* **100**, 7093 (1994).
- [10] A. Pinto, A. R. Pennisi, G. Faraci, G. D’Agostino, S. Mobilio, and F. Boscherini, *Phys. Rev. B* **51**, 5315 (1995).
- [11] M. M. Alvarez, J. T. Khoury, T. G. Schaaff, M. Shafigullin, I. Vezmar, and R. L. Whetten, *Chem. Phys. Lett.* **266**, 91 (1997).
- [12] T. G. Schaaff, M. N. Shafigullin, J. T. Khoury, I. Vezmar, R. L. Whetten, W. G. Cullen, P. N. First, C. Gutiérrez-Wing, J. Ascensio, and M. J. Jose-Yacamán, *J. Phys. Chem. B* **101**, 7885 (1997).
- [13] C. L. Cleveland, U. Landman, M. N. Shafigullin, P. W. Stephens, and R. L. Whetten, *Z. Phys. D* **40**, 503 (1997).
- [14] K. Koga, H. Takeo, T. Ikeda, and K. Ohshima, *Phys. Rev. B* **57**, 4053 (1998).
- [15] B. Palpant, B. Prével, J. Lermé, E. Cottancin, M. Pellarin, M. Treilleux, A. Perez, J. L. Vialle, and M. Broyer, *Phys. Rev. B* **57**, 1963 (1998).
- [16] L. E. Harrell, T. P. Bigioni, W. G. Cullen, R. L. Whetten, and P. N. First, *J. Vac. Sci. Technol. B* **17**, 2411 (1999).
- [17] V. A. Spasov, Y. Shi, and K. M. Ervin, *Chem. Phys.* **262**, 75 (2000).
- [18] M. Vogel, K. Hansen, A. Herlert, and L. Schweikhard, *Eur. Phys. J. D* **16**, 73 (2001).
- [19] N. Vandamme, G. Verschoren, A. Depuydt, M. Cannaerts, W. Bouwen, P. Lievens, R. E. Silverans, C. V. Haesendonck, *Appl. Phys. A* **72**, 177 (2001).

- [20] H. Hövel, Appl. Phys. A **72**, 295 (2001).
- [21] V. Torma, O. Vidoni, U. Simon, and G. Schmid, Eur. J. Inorg. Chem. 1121 (2003).
- [22] R. Salvati, A. Longo, G. Carotenuto, L. Nicolais, S. De Nicola, and G. P. Pepe, Eur. Phys. J. B **41**, 43 (2004).
- [23] G. Mills, B. Wang, W. Ho, and H. Metiu, J. Chem. Phys. **120**, 7738 (2004).
- [24] B. K. Min, W. T. Wallace, A. K. Santra, and D. W. Goodman, J. Phys. Chem. B **108**, 16339 (2004).
- [25] H. Häkkinen, M. Moseler, O. Kostko, N. Morgner, M. A. Hoffmann, and B. v. Issendorff, Phys. Rev. Lett. **93**, 093401 (2004).
- [26] L. Lamare and F. Michel-Calendini, Int. J. Quant. Chem. **61**, 635 (1997).
- [27] O. D. Häberlen, S. - C. Chung, M. Stener, and N. Rösch, J. Chem. Phys. **106**, 5189 (1997).
- [28] G. Bravo-Pérez, I. L. Garzón, and O. Novaro, J. Mol. Str. (Theochem) **493**, 225 (1999).
- [29] H. Häkkinen, R. N. Barnett, and U. Landman, Phys. Rev. Lett. **82**, 3264 (1999).
- [30] H. Grönbeck and W. Andreoni, Chem. Phys. **262**, 1 (2000).
- [31] H. Häkkinen and U. Landman, Phys. Rev. B **62**, 2287(R) (2000).
- [32] J. M. Soler, M. R. Beltrán, K. Michaelian, I. L. Garzón, P. Ordejón, D. Sánchez-Portal, and E. Artacho, Phys. Rev. B **61**, 5771 (2000).
- [33] H. Häkkinen, M. Moseler, and U. Landman, Phys. Rev. Lett. **89**, 033401 (2002).
- [34] J. Olviedo and R. E. Palmer, J. Chem. Phys. **117**, 9548 (2002).
- [35] J. Wang, G. Wang, and J. Zhao, Phys. Rev. B **66**, 035418 (2002).
- [36] J. Wang, G. Wang, and J. Zhao, Chem. Phys. Lett. **380**, 716 (2003).
- [37] J. Zhao, J. Wang, and J. G. Hou, Phys. Rev. B **67**, 085404 (2003).
- [38] B. Yoon, H. Häkkinen, and U. Landman, J. Phys. Chem. A **107**, 4066 (2003).
- [39] M. P. Johansson, D. Sundholm, and J. Vaara, Angew. Chem. Int. Ed. **43**, 2678 (2004).

- [40] S. Chrétien, M. S. Gordon, H. Metiu, J. Chem. Phys. **121**, 3756 (2004).
- [41] R. M. Olson, S. Varganov, M. S. Gordon, H. Metiu, S. Chretien, P. Piecuch, K. Kowalski, S. A. Kucharski, and M. Musia, J. Am. Chem. Soc. **127**, 1049 (2005).
- [42] L. Xiao and L. Wang, Chem. Phys. Lett. **392**, 452 (2004).
- [43] A. V. Walker, J. Chem. Phys. **122**, 094310 (2005).
- [44] F. Remacle and E. S. Kryachko, J. Chem. Phys. **122**, 044304 (2005).
- [45] H. Häkkinen, B. Yoon, U. Landman, X. Li, H.-J. Zhai, and L.-S. Wang, J. Phys. Chem. A **107**, 6168 (2003).
- [46] S. Gilb, P. Weis, F. Furche, R. Ahlrichs, and M. M. Kappes, J. Chem. Phys. **116**, 4094 (2002).
- [47] F. Furche, R. Ahlrichs, P. Weis, C. Jacob, S. Gilb, T. Bierweiler, and M. M. Kappes, J. Chem. Phys. **117**, 6982 (2002).
- [48] M. Neumaier, F. Weigend, and O. Hampe, J. Chem. Phys. **122**, 104702 (2005).
- [49] F. Ercolessi, W. Andreoni, and E. Tosatti, Phys. Rev. Lett. **66**, 911 (1991).
- [50] H. Arslan and M. H. Güven, Springer-Verlag, ARI (1998) **51**, 145
- [51] W. D. Luedtke and U. Landman, J. Phys. Chem. B **102**, 6566 (1998).
- [52] C. L. Cleveland, W. D. Luedtke, and U. Landman, Phys. Rev. Lett. **81**, 2036 (1998).
- [53] C. L. Cleveland, W. D. Luedtke, and U. Landman, Phys. Rev. B **60**, 5065 (1999).
- [54] Y. Chushak and L. S. Bartell, Eur. Phys. J. D **16**, 43 (2001).
- [55] S. M. Paik, S. M. Yoo, M. Namkung, and R. A. Wincheski, NASA/CR-2001-211014, ICASE Report No. 2001-17
- [56] S. -C. Lee, K. -R. Lee, J. -G. Lee, and N. M. Hwang, Nanotech Vol. 2 (2002).
- [57] F. Baletto, R. Ferrando, A. Fortunelli, F. Montalenti, C. Mottet, J. Chem. Phys. **116**, 3856 (2002).
- [58] J. Rogan, R. Ramírez, A. H. Romero, and M. Kiwi, Eur. Phys. J. D **28**, 219 (2004).

- [59] U. Landman and W. D. Luedtke, *Faraday Discuss.* **125**, 1 (2004).
- [60] Y. Wang, S. Teitel, and C. Dellago, *J. Chem. Phys.* **122**, 214722 (2005).
- [61] C. L. Cleveland, U. Landman, T. G. Schaaff, M. N. Shafigullin, P. W. Stephens, and R. L. Whetten, *Phys. Rev. Lett.* **79**, 1873 (1997).
- [62] R. N. Barnett, C. L. Cleveland, H. Häkkinen, W. D. Luedtke, C. Yannouleas, and U. Landman, *Eur. Phys. J. D* **9**, 95 (1999).
- [63] J. P. K. Doye and D. J. Wales, *New J. Chem.* **22**, 733 (1998).
- [64] N. T. Wilson and R. L. Johnston, *Eur. Phys. J. D* **12**, 161 (2000).
- [65] N. T. Wilson and R. L. Johnston, *Phys. Chem. Chem. Phys.* **4**, 4168 (2002).
- [66] I. L. Garzón and A. Posada-Amarillas, *Phys. Rev. B* **54**, 11796 (1996).
- [67] I. L. Garzón, K. Michaelian, M. R. Beltrán, A. Posada-Amarillas, P. Ordejón, E. Artacho, D. Sánchez-Portal, and J. M. Soler, *Phys. Rev. Lett.* **81**, 1600 (1998).
- [68] I. L. Garzón, K. Michaelian, M. R. Beltrán, A. Posada-Amarillas, P. Ordejón, E. Artacho, D. Sánchez-Portal, and J. M. Soler, *Eur. Phys. J. D* **9**, 211 (1999).
- [69] K. Michaelian, N. Rendón, and I. L. Garzón, *Phys. Rev. B* **60**, 2000 (1999).
- [70] T. X. Li, S. Y. Yin, Y. L. Ji, B. L. Wang, G. H. Wang, and J. J. Zhao, *Phys. Lett. A* **267**, 403 (2000).
- [71] S. Darby, T. V. Mortimer-Jones, R. L. Johnston, and C. Roberts, *J. Chem. Phys.* **116**, 1536 (2002).
- [72] C. Rey, L. J. Gallego, J. García - Rodeja, J. A. Alonso, and M. P. Iñiguez, *Phys. Rev. B* **48**, 8253 (1993).
- [73] J. García - Rodeja, C. Rey, L. J. Gallego, and J. A. Alonso, *Phys. Rev. B* **49**, 8495 (1994).
- [74] A. Sebetci and Z. B. Güvenç, *Modelling Simul. Mater. Sci. Eng.* **13**, 683 (2005).
- [75] M. S. Daw and M. I. Baskes, *Phys. Rev. Lett.* **50**, 1285 (1983).
- [76] M. S. Daw and M. I. Baskes, *Phys. Rev. B* **29**, 6443 (1984).

- [77] S. M. Foiles, M. I. Baskes, and M. S. Daw, Phys. Rev. B **33**, 7983 (1986).
- [78] A. F. Voter and S. P. Chen, in *Characterization of Defects in Materials*, edited by R. W. Siegal, J. R. Weertman, and R. Sinclair, MRS Symposia Proceedings No. 82 (Materials Research Society, Pittsburgh, 1987), p. 175.
- [79] A. Voter, Los Alamos Unclassified Technical Report No LA-UR 93-3901 (1993).
- [80] A. F. Voter, in *Intermetallic Compounds*, edited by J. H. Westbrook and R. L. Fleischer (John Wiley and Sons, Ltd, 1995), Vol. 1, p. 77.
- [81] V. G. Grigoryan, D. Alamanova, and M. Springborg, Eur. Phys. J. D **34**, 187 (2005).
- [82] D. Alamanova, Y. Dong, H. ur-Rehman, M. Springborg, and V. G. Grigoryan, Computing Letters (in press)
- [83] W. H. Press, S. A. Teukolsky, W. T. Vetterling, B. P. Flannery, in *Numerical Recipes in FORTRAN: the Art of Scientific Computing*, (Cambridge University Press, Cambridge, 1992), p. 387.
- [84] V. G. Grigoryan and M. Springborg, Chem. Phys. Lett. **375**, 219 (2003).
- [85] V. G. Grigoryan and M. Springborg, Phys. Rev. B **70**, 205415 (2004).

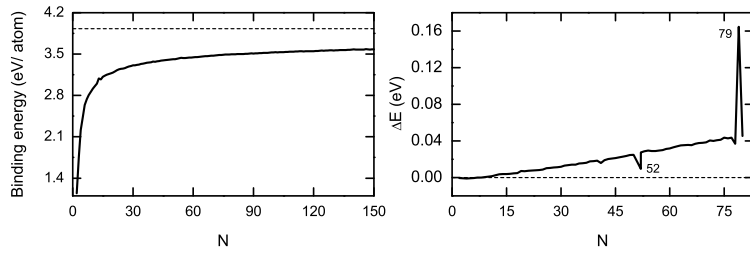


Figure 1: On the left we show the binding energy per atom as a function of size for the energetically lowest isomers of N up to 150 with the dashed line giving the *bulk* value; on the right is displayed the difference between the total energies of the lowest-lying isomers with up to 80 atoms obtained by Sebetci *et al.* and those found here, using different structure-optimization methods but the same embedded-atom approach.

Table 1: Point groups of the optimized gold clusters. $N.k$ marks the energetically k -lowest isomer of the Au_N cluster.

N	N.1	N.2	N.3	N	N.1	N.2	N.3	N	N.1	N.2	N.3
2	$D_{\infty h}$			51	C_1	C_1	C_1	101	C_2	D_{5h}	C_1
3	D_{3h}			52	D_{5d}	C_{2v}	C_{2v}	102	C_1	C_1	C_1
4	T_d			53	C_{5v}	C_{3v}	C_1	103	C_2	C_2	C_1
5	D_{3h}			54	I_h	C_1	C_s	104	C_1	C_2	C_1
6	O_h	C_{2v}		55	C_{3v}	C_s	C_1	105	C_2	C_s	C_2
7	D_{5h}	C_{3v}	C_2	56	C_s	C_{2v}	C_2	106	C_{3v}	C_1	C_s
8	D_{2d}	C_s	D_{3d}	57	C_1	C_1	C_1	107	C_s	C_1	C_1
9	C_{2v}	D_{3h}	C_s	58	C_1	C_s	C_1	108	C_s	C_s	C_1
10	C_{3v}	D_{4d}	D_{3h}	59	C_s	C_1	C_1	109	C_{3v}	C_1	C_1
11	C_{2v}	C_2	C_2	60	C_s	C_s	C_1	110	C_{2v}	C_1	C_1
12	C_{5v}	C_2	D_{3h}	61	C_{3v}	C_s	C_{2v}	111	C_1	C_1	C_1
13	I_h	C_1	C_s	62	C_s	C_1	C_1	112	C_{2v}	C_1	C_1
14	C_{3v}	C_{2v}	C_s	63	C_{2v}	C_s	C_s	113	T	C_2	D_2
15	D_{6d}	C_{2v}	C_s	64	C_{2v}	C_1	C_s	114	C_3	C_{2v}	C_2
16	C_{2v}	D_{3h}	C_{2v}	65	C_1	C_1	C_1	115	C_s	C_1	C_s
17	T_d	D_{4d}	C_s	66	C_s	C_2	C_1	116	C_s	O_h	C_{3v}
18	C_{4v}	C_{2v}	C_s	67	C_s	C_1	C_1	117	C_s	C_s	C_1
19	D_{5h}	D_{4d}	C_{2v}	68	C_s	C_1	C_1	118	C_{2v}	C_1	C_1
20	D_{3d}	D_2	D_{2h}	69	C_2	C_1	C_1	119	C_1	C_1	C_1
21	C_s	C_1	C_s	70	C_1	C_1	C_1	120	C_1	C_1	C_1
22	C_1	C_s	D_{6h}	71	C_{2v}	C_{2v}	C_1	121	C_1	C_1	C_1
23	C_{2v}	C_s	C_s	72	C_s	C_s	C_s	122	C_1	C_1	C_1
24	C_2	C_s	C_{3v}	73	C_{2v}	C_1	C_s	123	C_s	C_1	C_1
25	C_2	C_1	C_{2v}	74	C_s	C_{5v}	C_s	124	C_s	C_1	C_s
26	C_1	C_s	C_s	75	D_{5h}	C_{2v}	C_s	125	C_1	C_1	C_1
27	C_s	C_2	C_s	76	C_s	C_s	C_s	126	C_s	C_1	C_1
28	C_s	C_2	C_{2v}	77	C_{2v}	C_s	C_{2v}	127	C_1	C_1	C_1
29	C_2	C_s	C_2	78	C_{2v}	C_s	C_1	128	C_s	C_1	C_s
30	C_{3v}	C_1	C_2	79	O_h	C_s	C_1	129	C_1	C_s	C_s
31	C_3	C_1	C_{3v}	80	C_s	O	C_s	130	C_s	C_s	C_s
32	D_{2d}	C_3	C_{2v}	81	C_{2v}	C_s	C_1	131	C_{2v}	C_1	C_1
33	C_2	C_1	C_1	82	C_s	C_3	C_{2v}	132	C_s	C_1	C_1
34	T_d	C_3	C_s	83	C_s	C_s	C_s	133	C_{2v}	C_1	C_1
35	C_{2v}	D_3	C_{2v}	84	C_s	C_s	C_s	134	C_s	C_s	C_s
36	C_{2v}	C_s	D_2	85	C_s	C_s	C_s	135	C_s	C_1	C_1
37	C_{2v}	C_s	C_2	86	C_s	C_s	C_s	136	C_s	C_1	C_1
38	O_h	D_{4h}	C_s	87	C_2	C_1	C_1	137	C_{2v}	C_1	C_1
39	D_3	C_s	C_{4v}	88	C_1	C_1	C_1	138	C_s	C_1	C_1
40	D_3	C_1	C_2	89	C_2	C_s	C_s	139	C_{2v}	C_1	C_1
41	C_1	C_1	C_1	90	C_1	C_1	C_1	140	O_h	C_s	C_s
42	D_4	T_d	C_1	91	C_1	C_1	C_1	141	C_{2v}	C_{2v}	C_s
43	D_2	C_1	C_1	92	C_1	C_2	C_1	142	C_s	C_s	C_s
44	C_s	C_2	C_1	93	C_1	C_1	C_1	143	C_s	C_{2v}	C_s
45	C_s	C_1	C_1	94	C_{20}	C_1	C_1	144	C_s	C_s	C_s
46	C_3	C_s	C_1	95	C_1	C_1	C_1	145	C_1	C_s	C_1
47	C_1	C_2	C_1	96	C_1	C_1	C_1	146	D_{5h}	C_s	C_1
48	C_1	D_{2d}	C_1	97	C_2	C_1	C_1	147	C_1	C_1	C_1
49	C_1	C_1	C_s	98	C_1	C_1	C_1	148	C_1	C_1	C_1
50	C_1	C_1	C_1	99	C_2	C_1	C_1	149	C_1	C_1	C_1
				100	C_1	C_1	C_1	150	C_1	C_1	C_1

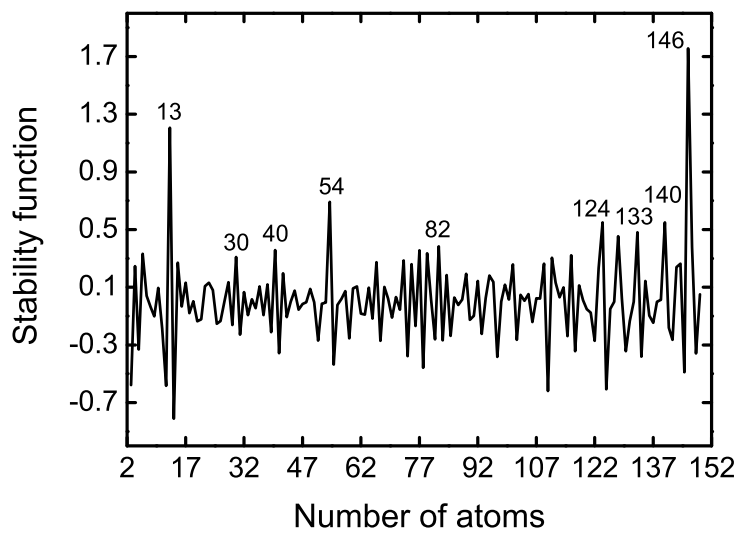


Figure 2: The stability function as a function of cluster size.

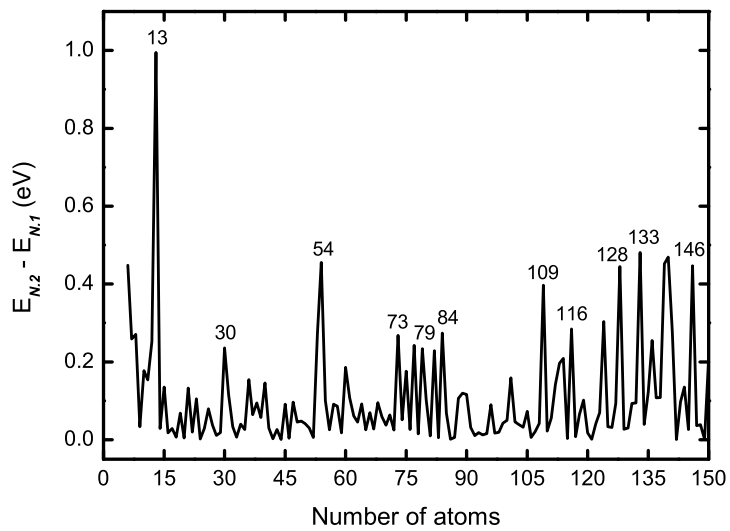


Figure 3: The total-energy difference between the two energetically lowest neighbouring isomers as a function of cluster size.

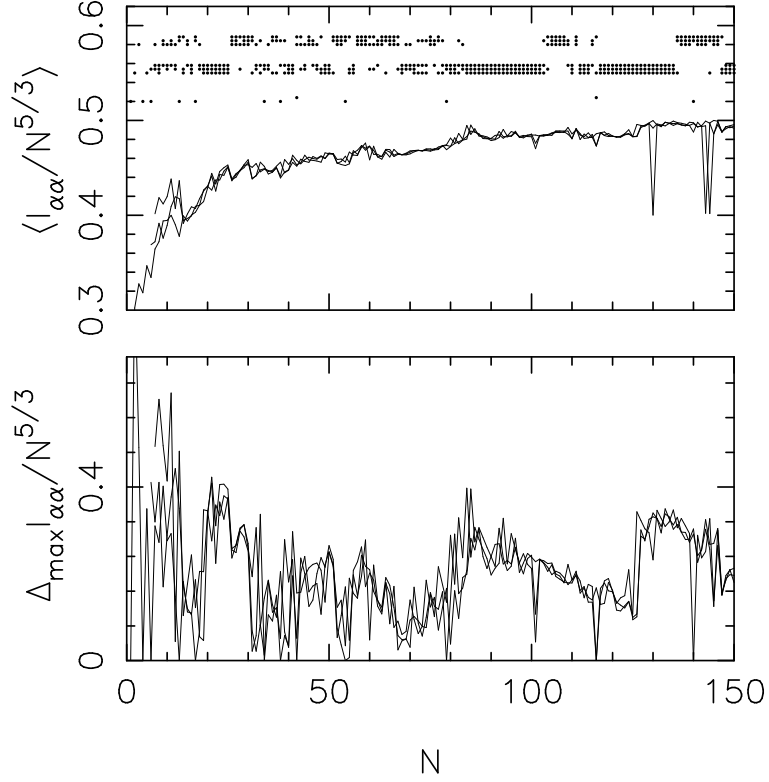


Figure 4: Different properties related to the eigenvalues $I_{\alpha\alpha}$ of the matrix with the moments of inertia. In the upper panel we show the average value together with points indicating whether clusters with overall spherical shape (lowest set of rows), overall cigar shape (middle set of rows), or overall lens shape (upper set of rows) are found for a certain size. Moreover, in each set of rows, the lowest row corresponds to the energetically lowest isomer, the second one to the energetically second-lowest isomer, etc. In the lower panel we show the maximum difference of the eigenvalues for the three different isomers.

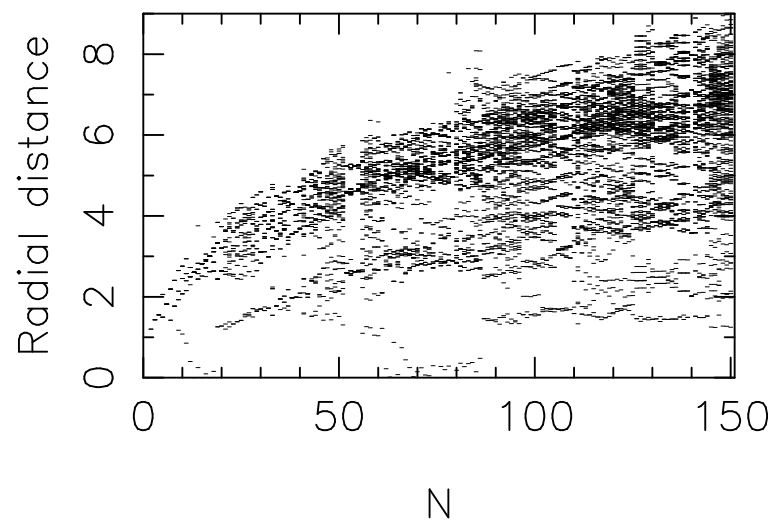


Figure 5: The distribution of radial distances (in Å) for the lowest-lying isomer as a function of cluster size. Each small line represents (at least) one atom with that radial distance.

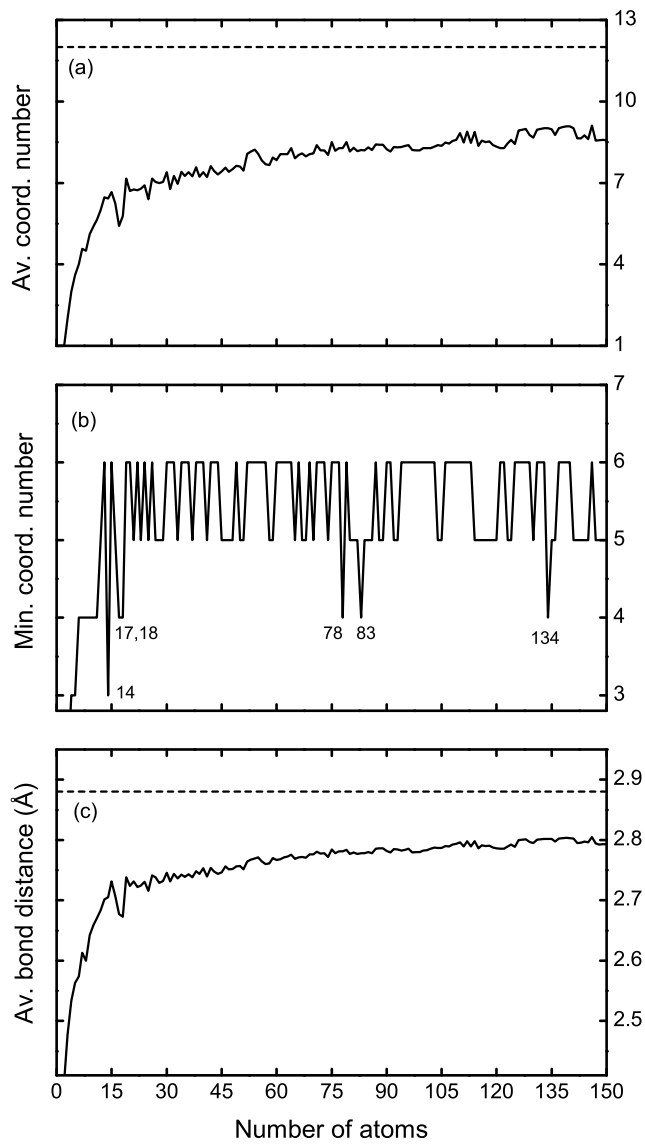


Figure 6: (a) the average coordination number, (b) the minimum coordination number, and (c) the average bond length as functions of cluster size. The dashed lines in (a) and (c) show the corresponding bulk values for gold.

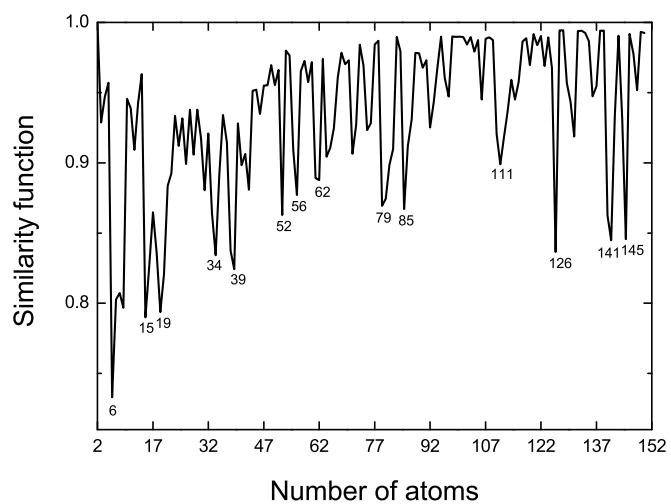


Figure 7: The similarity function as function of cluster size. It describes whether the cluster with N atoms is similar to that of $N - 1$ atoms plus an extra atom.

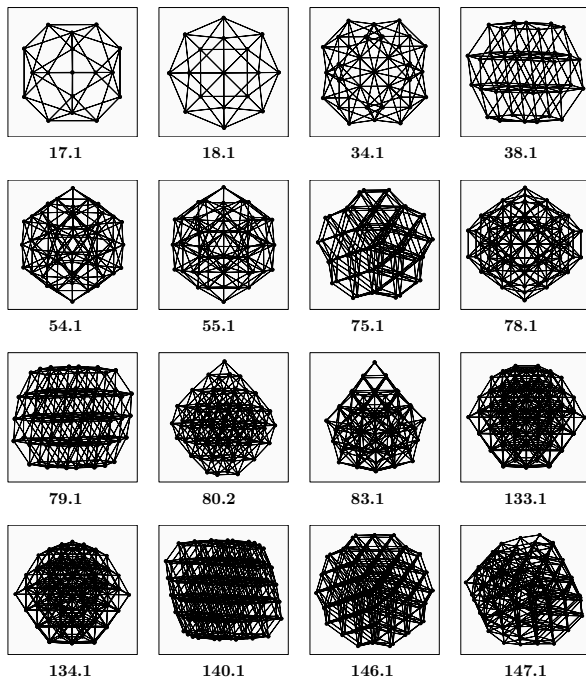


Figure 8: Some Au_N clusters with high or peculiar symmetry.